

# Generation of sub-6-fs blue pulses by frequency doubling with quasi-phase-matching gratings

L. Gallmann, G. Steinmeyer, and U. Keller

*Ultrafast Laser Physics Laboratory, Institute of Quantum Electronics, Swiss Federal Institute of Technology, ETH Hönggerberg-HPT, CH-8093 Zurich, Switzerland*

G. Imeshev and M. M. Fejer

*E. L. Ginzton Laboratory, Stanford University, Stanford, California 94305*

J.-P. Meyn

*FB Physik, Universität Kaiserslautern, D-67663 Kaiserslautern, Germany*

Received October 31, 2000

We demonstrate the generation of sub-6-fs pulses centered at 405 nm by frequency doubling of 8.6-fs Ti:sapphire laser pulses. The frequency doubling is carried out in a nonlinearly chirped quasi-phase-matching grating fabricated in a lithium tantalate substrate. This device simultaneously provides frequency conversion and pulse compression of the positively prechirped fundamental pulses. The second-harmonic pulses are characterized in a cross-correlation setup, and their pulse shapes are retrieved by two iterative phase-reconstruction algorithms. The generated second-harmonic spectrum spans a bandwidth of 220 THz. To our knowledge, these are the shortest pulses ever generated in the blue spectral region. © 2001 Optical Society of America  
*OCIS codes:* 370.7110, 320.5550, 190.4360.

Over the past decade there has been significant progress in the generation of ultrashort pulses in the visible and near-infrared spectral ranges.<sup>1</sup> Handling of such ultrashort pulses is challenging and requires careful compensation for dispersion. Transmission through a few millimeters of dielectric materials already causes significant pulse broadening. Frequency doubling of such ultrashort pulses poses additional problems. In particular, the group-velocity mismatch (GVM) between the first-harmonic (FH) and the second-harmonic (SH) pulses limits the length of the nonlinear crystal to typically less than  $\sim 50 \mu\text{m}$ . This crystal-length limitation poses practical problems of polishing and handling of such thin crystals. Recently, blue pulses with durations of 10 fs (Ref. 2) and 8 fs (Ref. 3) were generated by doubling of  $\sim 10$ -fs pulses from a Ti:sapphire oscillator by use of birefringent phase matching. In the latter experiment, focusing the FH tighter than confocally into a 100- $\mu\text{m}$ -thick BBO crystal reduced the effective interaction length and alleviated SH pulse broadening owing to GVM. 80 mW of SH light was generated, with 950-mW FH power and an efficiency of 0.7%/nJ.<sup>3</sup> In this Letter we describe an alternative approach to frequency doubling of sub-10-fs pulses that relies on the engineerability of quasi-phase-matching (QPM) gratings and does not suffer from crystal-length and focusing limitations. We demonstrate scalability to shorter pulse lengths by generating sub-6-fs blue pulses.

Microstructured QPM (Ref. 4) crystals have been used extensively in frequency-conversion devices and offer many advantages, such as noncritical phase matching, use of large nonlinearities, and tailoring

of the amplitude and phase response of the device, over conventional birefringent materials. A flexible approach to doubling sub-10-fs pulses is to use quasi-phase-matching second-harmonic generation (QPM-SHG) pulse compression. In the case of negligible material dispersion beyond the GVM, this pulse-compression technique relies on a combination of the GVM and spatial localization of conversion of different spectral components of the FH in a linearly chirped QPM grating.<sup>5,6</sup> If the chirp of the grating is chosen to match the chirp of a stretched FH pulse, the generated SH pulse is compressed, as was demonstrated for 100-fs-long pulses.<sup>7</sup> In this arrangement the grating length must be longer than the walk-off length by roughly the stretching ratio of the FH pulse, which is generally advantageous for short pulses because beam focusing and crystal polishing and handling become much less problematic with a long device. However, for sub-10-fs pulses group-velocity dispersion (GVD) and higher-order dispersion of the nonlinear medium become important, and a simple linearly chirped QPM grating does not compensate for dispersion correctly.<sup>8</sup> In this Letter we demonstrate the use of a QPM-SHG pulse compressor designed to account properly for material dispersion beyond the GVM to generate sub-6-fs blue pulses.

The first-order chirped QPM grating was fabricated in a 300- $\mu\text{m}$ -thick congruent lithium tantalate ( $\text{LiTaO}_3$ ) substrate by means of electric field poling.  $\text{LiTaO}_3$  was chosen instead of the more-common  $\text{LiNbO}_3$  because  $\text{LiTaO}_3$  has a deeper UV absorption edge, which makes two-photon absorption of the SH of less concern. The temporal walk-off length of 8.6-fs pulses at 810 nm is only  $\sim 6 \mu\text{m}$ . For

the  $\sim 20\times$ -stretched FH pulse used here, a chirped grating length of  $310\ \mu\text{m}$  was used to achieve pulse compression. The GVD coefficients of  $\text{LiTaO}_3$  are  $305\ \text{fs}^2/\text{mm}$  at the FH and  $1140\ \text{fs}^2/\text{mm}$  at the SH (Ref. 9), and hence GVD effects are substantial in the material length that was used. We designed the QPM grating according to the method reported in Ref. 8 to account for GVD and higher-order material dispersion. The chirp of the grating changed nonlinearly with propagation distance, covering QPM periods from  $6.5$  to  $1.8\ \mu\text{m}$ .<sup>10</sup> For this grating the expected conversion efficiency was  $\sim 2\%/n\text{J}$ , assuming confocal focusing and ideal poling quality.

The experimental setup for SH pulse generation and characterization is shown in Fig. 1. The pump source was a Kerr-lens mode-locked Ti:sapphire oscillator with a repetition rate of  $88\ \text{MHz}$  and average power of  $280\ \text{mW}$ .<sup>11</sup> The output from the oscillator passed through a stretcher composed of two identical broadband antireflection-coated fused-silica prisms (wedge angle,  $10^\circ$ ) separated by  $1\ \text{mm}$ . Variable insertion of the prisms provided an adjustable path length and hence positive chirp on the FH pulses without beam displacement. The beam was loosely focused into the chirped-period poled lithium tantalate (CPPLT) by a  $1.42\text{-mm}$ -thick,  $21\text{-mm}$  focal-length BK7 lens to a spot size of  $20\ \mu\text{m}$ . Owing to the compounded losses of the mirrors used for beam routing and the Fresnel reflection of the uncoated  $\text{LiTaO}_3$  sample, only  $\sim 90\ \text{mW}$  of the laser output arrived inside the CPPLT. The FH pulse acquired a total estimated chirp of  $\sim 180\ \text{fs}^2$  before entering the sample. The generated SH beam was collimated with a concave spherical aluminum-coated mirror of  $50\text{-mm}$  radius of curvature. The SH output power was  $0.41\ \text{mW}$  inside and  $0.35\ \text{mW}$  after the CPPLT, corresponding to an internal conversion efficiency of  $0.45\%/n\text{J}$ . The conversion efficiency is lower than the theoretical value of  $2\%/n\text{J}$  because of poling imperfections and the loose focusing employed.

For characterization of the generated SH pulses, cross correlation between the FH and SH pulses was used. For the FH reference pulse,  $8\%$  of the FH power was split off before the stretcher with a  $1\text{-mm}$ -thick fused-silica beam splitter oriented at  $45^\circ$  and passed through a delay line mounted on a piezo shaker. The SH beam and the FH reference beam were focused together by a concave  $30\text{-cm}$  radius-of-curvature aluminum-coated mirror into a  $<10\text{-}\mu\text{m}$ -thick KDP crystal. The generated sum-frequency signal near  $270\ \text{nm}$  passed through a Glan laser polarizer and an iris that rejected the SH and the FH light and was then detected by a solar-blind photomultiplier. The position of the piezo shaker was calibrated with He-Ne laser interference fringes in a separate Michelson interferometer.

Before measurement of the cross correlation, the chirp of the FH reference pulse was minimized at the location of the cross-correlation crystal, which was achieved by replacement of the cross-correlation crystal with a  $15\text{-}\mu\text{m}$ -thick ammonium dihydrogen phosphate crystal and adjustment of dispersion between the laser and the cross-correlation setup to

maximize the SH signal of the reference. Afterward, the dispersion of the prism stretcher before the CPPLT was adjusted for minimum cross-correlation width. The cross-correlation signal was recorded in a single sweep of the piezo shaker with an effective 11-bit digitization (Fig. 2). The FWHM of the trace shown in Fig. 2 is  $12.7\ \text{fs}$ .

The recorded SH spectrum had a bandwidth of  $220\ \text{THz}$  and a transform limit of  $4.8\ \text{fs}$  (Fig. 3). The measured SH spectral shape deviates from the theoretically expected SH spectrum, determined by the self-convolution of the FH spectrum, which we tentatively attribute to poling imperfections in the QPM structure. Such poling imperfections generally affect not the phase of the generated SH pulse but only its amplitude,<sup>8</sup> with the latter effect manifesting itself in the observed lower than ideal conversion efficiency. The origin of the rapidly varying spectral features is not fully understood but is not necessarily the QPM nature of the device, since a similar behavior was observed with birefringent phase matching.<sup>3</sup> We

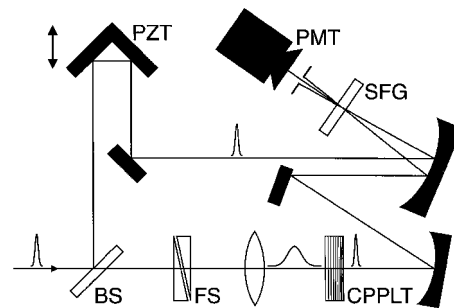


Fig. 1. Experimental setup for generation and characterization of SH pulses. Note the exclusive use of reflective optics for the reference beam and the doubling-crystal output. BS, beam splitter; FS, adjustable fused-silica wedges; PZT, piezo-driven translation stage; SFG, cross-correlation crystal; PMT, solar-blind photomultiplier.

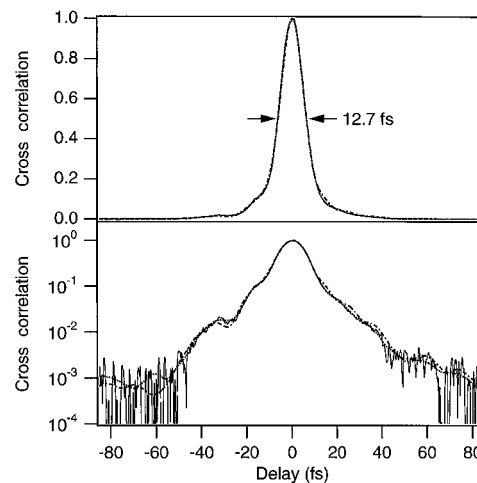


Fig. 2. Measured cross correlations (solid curves) on a linear (top) and a logarithmic scale (bottom). In addition to the measured data, the cross correlations reconstructed by the two algorithms described in the text are shown (dashed-dotted curve, algorithm 1; dotted curve, algorithm 2).

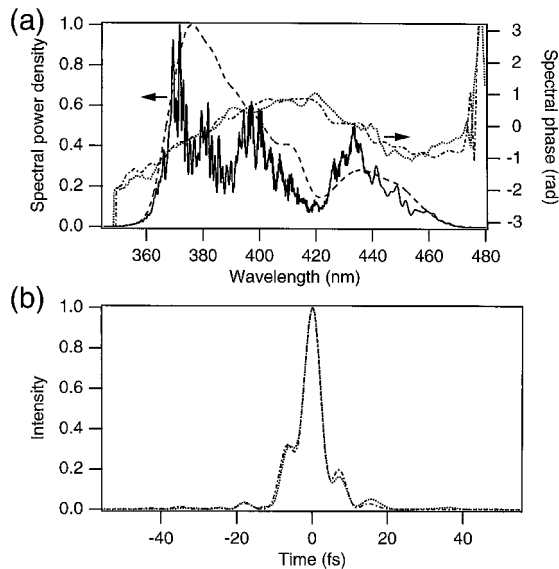


Fig. 3. Measured and reconstructed SH data (a) Measured SH power spectrum (solid curve) compared with the theoretically expected spectrum (dashed curve). The spectral phase of the SH pulse was consistently retrieved by use of the two decorrelation algorithms described in the text. (b) Both algorithms yield nearly identical SH pulse shapes corresponding to pulse durations of 5.2 fs for algorithm 1 (dashed-dotted curve) and 5.4 fs for algorithm 2 (dotted curve).

observed no indications of two-photon absorption or self-phase-modulation in the CPPLT.

The amplitude and phase of the SH pulse were retrieved from the cross correlation and the spectral data by use of two different iterative algorithms. Algorithm 1 used the cross correlation, the SH spectrum, and the temporal pulse shape of the FH reference pulse as the input. The reference pulse was measured by use of spectral phase interferometry for direct electric field reconstruction<sup>12,13</sup> and was found to have a FWHM duration of 8.6 fs and a transform limit of 8 fs. The multidimensional downhill simplex method was used to find the spectral phase of the SH pulse that minimizes the mean-square deviation between the reconstructed and measured cross-correlation functions. For algorithm 2, which is similar to an algorithm that was previously applied to intensity autocorrelation,<sup>14</sup> only the cross-correlation trace, the FH spectrum, and the SH spectrum served as input data. In this method the multidimensional optimization was applied to the FH and the SH spectral phase simultaneously. In both algorithms the spectral phases were initialized with random phase noise. The two algorithms delivered nearly identical pulse shapes (Fig. 3), which generally did not depend on the starting parameters. The FWHM durations of the retrieved SH pulses were 5.2 for algorithm 1 and 5.4 fs for algorithm 2. Occasionally we observed stagnation of the algorithm at a time-reversed version of the SH pulse. This case was readily identified by a higher mean-square deviation.

To the best of our knowledge, these sub-6-fs pulses generated by QPM-SHG pulse compression are the

shortest pulses ever reported in the blue spectral region. The setup is relatively simple and requires no critical alignment. We achieve stretching of the FH pulse simply by passing the pulse through an appropriate length of dispersive material. Other than the CPPLT, no element providing negative dispersion is needed to produce short SH pulses. The demonstrated approach allows scaling to even shorter blue pulses by use of shorter FH pulses, because there is no fundamental constraint on the crystal length. The FH pulses used in this experiment were relatively strongly chirped before entering the QPM grating. The efficiency of the SHG process scales with the FH peak power and can be improved by reduction of the FH chirp and by use of a QPM grating designed to generate a negatively chirped SH pulse. QPM grating designs based on an unchirped input pulse and the creation of a negatively chirped SH output to facilitate postcompression with a positive dispersion material promise efficiency that is an order of magnitude higher while retaining the simplicity of the current approach.

This research was supported by the Swiss National Science Foundation and by U.S. Air Force Office of Scientific Research grant F49620-99-1-0270. L. Gallmann's e-mail address is gallmann@iqe.phys.ethz.ch.

## References

1. G. Steinmeyer, D. H. Sutter, L. Gallmann, N. Matuschek, and U. Keller, *Science* **286**, 1507 (1999).
2. D. Steinbach, W. Hügel, and M. Wegener, *J. Opt. Soc. Am. B* **15**, 1231 (1998).
3. A. Fürbach, T. Le, C. Spielmann, and F. Krausz, *Appl. Phys. B* **70**, S37 (2000).
4. M. M. Fejer, G. A. Magel, D. H. Jundt, and R. L. Byer, *IEEE J. Quantum Electron.* **28**, 2631 (1992).
5. M. A. Arbore, O. Marco, and M. M. Fejer, *Opt. Lett.* **22**, 865 (1997).
6. G. Imeshev, M. A. Arbore, M. M. Fejer, A. Galvanauskas, M. Fermann, and D. Harter, *J. Opt. Soc. Am. B* **17**, 304 (2000).
7. M. A. Arbore, A. Galvanauskas, D. Harter, M. H. Chou, and M. M. Fejer, *Opt. Lett.* **22**, 1341 (1997).
8. G. Imeshev, M. A. Arbore, S. Kasriel, and M. M. Fejer, *J. Opt. Soc. Am. B* **17**, 1420 (2000).
9. J.-P. Meyn and M. M. Fejer, *Opt. Lett.* **22**, 1214 (1997).
10. The designed QPM grating period is approximated by  $\Lambda(z) = 7,725,550/(z - 3731.74) - 7,886,010/(z - 3800.3) + 30.76/(18.16 + z)$ , with  $\Lambda$  and  $z$  in micrometers.
11. D. H. Sutter, G. Steinmeyer, L. Gallmann, N. Matuschek, F. Morier-Genoud, U. Keller, V. Scheuer, G. Angelow, and T. Tschudi, *Opt. Lett.* **24**, 631 (1999).
12. C. Iaconis and I. A. Walmsley, *Opt. Lett.* **23**, 792 (1998).
13. L. Gallmann, D. H. Sutter, N. Matuschek, G. Steinmeyer, U. Keller, C. Iaconis, and I. A. Walmsley, *Opt. Lett.* **24**, 1314 (1999).
14. A. Baltuska, A. Pugzlys, M. S. Pshenichnikov, and D. A. Wiersma, in *Digest of Conference on Lasers and Electro-Optics 2000 OSA Technical Digest Series* (Optical Society of America, Washington, D.C., 1999), paper CWF22.